Dartmouth College

Dartmouth Digital Commons

Dartmouth Scholarship

Faculty Work

3-9-2011

Coherent-State Transfer Via Highly Mixed Quantum Spin Chains

Paola Cappellaro
Massachusetts Institute of Technology

Lorenza Viola
Dartmouth College

Chandrasekhar Ramanathan
Dartmouth College

Follow this and additional works at: https://digitalcommons.dartmouth.edu/facoa

Part of the Engineering Commons, and the Quantum Physics Commons

Dartmouth Digital Commons Citation

Coherent-state transfer via highly mixed quantum spin chains

Paola Cappellaro

Nuclear Science and Engineering Department, Massachusetts Institute of Technology, Cambridge, Massachusetts 02139, USA

Lorenza Viola and Chandrasekhar Ramanathan

Department of Physics and Astronomy, Dartmouth College, 6127 Wilder Laboratory, Hanover, New Hampshire 03755, USA

Spin chains have been proposed as quantum wires in many quantum-information processing architectures. Coherent transmission of quantum information in spin chains over short distances is enabled by their internal dynamics, which drives the transport of single-spin excitations in perfectly polarized chains. Given the practical challenge of preparing the chain in a pure state, we propose to use a chain that is initially in the maximally mixed state. We compare the transport properties of pure and mixed-state chains and find similarities that enable the experimental study of pure-state transfer via mixed-state chains. We also demonstrate protocols for the perfect transfer of quantum information in these chains. Remarkably, mixed-state chains allow the use of Hamiltonians that do not preserve the total number of single-spin excitations and are more readily obtainable from the naturally occurring magnetic dipolar interaction. We discuss experimental implementations using solid-state nuclear magnetic resonance and defect centers in diamond.

I. INTRODUCTION

Many quantum-information processing (QIP) proposals require the computational units to be spatially separated due to constraints in fabrication or control [1–3]. Coherent information transfer from one quantum register to another must then be carried out either by photons or, for more compact architectures, by quantum wires. Linear chains of spins have been proposed as quantum wires, the desired transport being obtained via the free evolution of the spins under their mutual interaction [4–9]. In general, only partial control over the spins in the chain is assumed, as relevant to most experimental implementations, and perfect state transfer with reduced or no control requirements has already been studied [10–12].

Reduced control may also naturally entail an imperfect initialization of the spin chain in a state other than the intended one, possibly mixed. With some notable exceptions (e.g., [12–15]), where protocols for perfect state transfer without state initialization have been investigated under the assumption of sufficient end-chain control, existing analyses have primarily focused on transport in the one-spin excitation manifold. However, imperfect chain initialization makes it imperative to more systematically study the transport properties of the higher excitation manifolds in order to both obtain a general characterization of the dynamics of mixed-state spin chains under different physical Hamiltonians and possibly further relax the required control resources.

In this paper we focus on the transport properties of chains that are initially in the *maximally mixed state*. This state corresponds to the infinite temperature limit and is easily reachable for many systems of relevance to QIP [16–18]. Alternatively, it could be obtained by an active randomization of the chain's initial state. The reduced requirements on the initialization of the wires, when combined with low control requirements, would make quantum-information transport more accessible to experimental implementations. We are thus interested in comparing the transport properties of pure and mixed-state chains with a twofold goal in mind: (i) exploring

the extent to which the experimental study of pure-state transport may be enabled by its simulation via highly mixed chains, and (ii) studying protocols for the transport of quantum information via mixed-state chains.

The paper is organized as follows. We first review in Sec. II some results regarding transport in the one-spin excitation manifold and then generalize them to higher excitation manifolds and mixed states. Furthermore, we describe how transport may also be driven by Hamiltonians that do not conserve the number of single-spin excitations. In Sec. III we investigate transfer of quantum information in a mixed-state chain based on a standard encoding protocol [14] and extend it to more general Hamiltonians. In Sec. IV we then present applications of these results, focusing on two experimental QIP platforms. The first is based on solid-state nuclear magnetic resonance (NMR) and enables the study of transport in mixed-state chains and its limitations due to imperfections in the system [7,19,20]. The second example is an application of quantum-information transfer via mixed-state wires in a scalable architecture based on spin defects in diamond [21–23].

II. STATE TRANSFER IN PURE- AND MIXED-STATE SPIN CHAINS

A. Single-spin excitation manifold

In analogy with the phenomenon of spin waves, the simplest mechanism for quantum-state transfer is the propagation of a single-spin excitation $|j\rangle = |00\ldots01_j0\ldots\rangle$ down a chain of n spins-1/2, coupled by the Heisenberg exchange Hamiltonian [4,24]. In this context, the most common model studied is the *XX* model, described by the Hamiltonian

$$\mathcal{H}_{XX} = \sum_{j=1}^{n-1} \frac{d_j}{2} \left(\sigma_x^j \sigma_x^{j+1} + \sigma_y^j \sigma_y^{j+1}\right), \quad (1)$$

where σ_α ($\alpha = \{x,y,z\}$) are the Pauli matrices, d_j the couplings, and we have set $\hbar = 1$. A single-spin excitation

is propagated through the chain via energy-conserving spin flip-flops, as shown by rewriting the *XX* Hamiltonian in terms of the operators $\sigma_\pm = (\sigma_x \pm i\sigma_y)/2$:

$$\mathcal{H}_{XX} = \sum_{j=1}^{n-1} d_j(\sigma_+^j \sigma_-^{j+1} + \sigma_-^j \sigma_+^{j+1}). \quad (2)$$

The transport properties of the *XX* Hamiltonian are made apparent by a mapping of the system to a local fermionic Hamiltonian via the Jordan-Wigner transformation,

$$c_j = \prod_{k=1}^{j-1}\left(-\sigma_z^k\right)\sigma_-^j, \quad \sigma_-^j = \prod_{k=1}^{j-1}(1/2 - c_k^\dagger c_k)c_j, \quad (3)$$

which also yields $\sigma_z^j = 1 - 2c_j^\dagger c_j$. Using these fermion operators, the *XX* Hamiltonian can be rewritten as

$$\mathcal{H}_{XX} = \sum_{j=1}^{n-1} d_j(c_j^\dagger c_{j+1} + c_{j+1}^\dagger c_j). \quad (4)$$

Since the total angular momentum along z, $Z = \sum_{j=1}^n \sigma_z^j$, is conserved, $[\mathcal{H}_{XX}, Z] = 0$, it is possible to block-diagonalize the Hamiltonian into subspaces corresponding to (typically degenerate) eigenvalues of Z. These subspaces are more simply characterized by the number of spins in the excited state $|1\rangle$, which is usually called the (magnon) excitation number. In this description, the *XX* Hamiltonian induces transport by creating an excitation at site $j + 1$ while annihilating another at site j. For a given evolution time $t > 0$, transport from spin j to spin l is characterized by the transfer fidelity of the state $|j\rangle$ to $|l\rangle$, defined as the overlap $P_{jl}^{XX}(t) = |A_{jl}(t)|^2 = |\langle l|U_{XX}(t)|j\rangle|^2$, where $U_{XX}(t) = e^{-i\mathcal{H}_{XX}t}$ and usually $j = 1$ and $l = n$ in a open-ended chain.

A well-studied case [5–7] is the *homogenous* limit, corresponding to equal couplings, $d_j = d$ for all j. The corresponding Hamiltonian can be diagonalized by the operators

$$a_k^h = \frac{1}{\sqrt{n+1}} \sum_{j=1}^n \sin(\kappa j)c_j, \quad \kappa = \frac{\pi k}{n+1}, \quad k = 1, \dots, n,$$

to reveal the eigenvalues $\omega_k^h = 2d\cos(\kappa)$. It is then possible to calculate the probability of state transfer from spin j to spin l, yielding $P_{jl}^{h,XX}(t) = |A_{jl}^h(t)|^2$, with [5]:

$$A_{jl}^h(t) = \frac{2}{n+1} \sum_k \sin(\kappa j) \sin(\kappa l)e^{-i\omega_k t}. \quad (5)$$

In practice, it is often difficult to experimentally prepare the spins in the maximally polarized, ground state. Thus, in order to experimentally investigate quantum transport, it is highly desirable to relax the requirements on the initial state of the spin chain. In [7] we found that it was possible to simulate the spin excitation transport by using a highly mixed spin chain. We generalized the spin excitation transport to mixed states by looking at the evolution of an initial state of the form

$$\rho = \frac{1}{2^n}\left(\mathbb{1} + \epsilon \delta\rho_z^j\right), \quad \delta\rho_z^j = \mathbb{1}_{j-1} \otimes \sigma_z^j \otimes \mathbb{1}_{n-j}.$$

This state represents a completely mixed state chain with a single spin partially polarized along the z axis. A metric

that quantifies the efficiency with which the initial state is transferred from spin j to spin l is given by the correlation between the resulting time-evolved state and the intended final state, that is, $M_{jl}(t) = \text{Tr}\{\rho_j(t)\rho_l\}$. Notice, however, that as long as the dynamics is unital, we only need to follow the evolution of the traceless deviation $\delta\rho$ from the identity; thus, in what follows we often use a simplified metric defined as $C_{jl}(t) = \text{Tr}\{\delta\rho_z^j(t)\delta\rho_z^l\}$. Using a fermionic mapping of the mixed states, we found in Ref. [7] that for the homogenous *XX* Hamiltonian such a correlation is *exactly* given by $P_{jl}^{h,XX}(t)$, although the states involved in the transport are quite different. Indeed, states such as $\delta\rho_z^j$ do not reside in the lowest excitation manifold, for which the state transfer Eq. (5) was initially calculated, but they are a mixture spanning all the possible excitation manifolds.

A similar mapping from mixed to pure states cannot be carried further in such a simple way. For example, we cannot use the state $\delta\rho_x^j = \mathbb{1}_{j-1} \otimes \sigma_x^j \otimes \mathbb{1}_{n-j}$ to simulate the transfer of a coherent pure state such as $|+\rangle|00\dots\rangle$, where $|+\rangle = (|0\rangle + |1\rangle)/\sqrt{2}$.

In the following, we analyze the conditions allowing state transfer in mixed-state spin chains in order to lay the basis of a protocol for the transport of quantum information.

B. Evolution in higher excitation manifolds

Since highly mixed states include states with support in all the spin excitation manifolds, we first analyze the evolution of higher excitation energy eigenstates. Thanks to the fact that it conserves the spin excitation number, the *XX* Hamiltonian [Eq. (1)] can be diagonalized in each excitation subspace. Let the eigenstates in the first excitation subspace be denoted by $|E_k\rangle$ (e.g., $|E_k\rangle = \sqrt{\frac{2}{n+1}} \sum_j \sin(\kappa j)|j\rangle$ in the homogeneous case). Since the *XX* Hamiltonian describes noninteracting fermions, eigenfunctions of the higher manifolds can be exactly expressed in terms of Slater determinants of the one-excitation manifold. Consider, for example, the case of the two-excitation manifold, described by states $|pq\rangle = |0\dots1_p\dots0\dots1_q\dots0\rangle$. The eigenstates $|E_{kh}\rangle$ are

$$|E_{kh}\rangle = \frac{1}{2} \sum_{pq} \left(\langle E_k|p\rangle\langle E_h|q\rangle - \langle E_k|q\rangle\langle E_h|p\rangle\right)|pq\rangle, \quad (6)$$

with eigenvalues $E_{kh} = E_k + E_h$. We can then calculate the time evolution as

$$U_{XX}(t)|pq\rangle = \sum_{k,h} e^{-i(\omega_k+\omega_h)t}\langle E_{kh}|pq\rangle\langle rs|E_{kh}\rangle|rs\rangle$$

$$= \sum_{r,s} A_{pq,rs}(t)|rs\rangle,$$

where

$$A_{pq,rs}(t) = \begin{vmatrix} A_{pr}(t) & A_{ps}(t) \\ A_{qr}(t) & A_{qs}(t) \end{vmatrix}, \quad (7)$$

and $A_{pr}(t)$ describes the amplitude of the transfer in the one-excitation manifold, $A_{pr}(t) = \langle r|U_{XX}|p\rangle$.

More generally, for an arbitrary initial eigenstate of Z, $|\vec{p}\rangle = |p_1, p_2, \dots\rangle$, with $p_k \in \{0,1\}$, the transfer amplitude to

the eigenstate $|\vec{r}\rangle$ is given by

$$
A_{\vec{p}\vec{r}}(t) = \begin{vmatrix} A_{p_1 r_1}(t) & A_{p_1 r_2}(t) & \dots \\ A_{p_2 r_1}(t) & A_{p_2 r_2}(t) & \dots \\ \dots & \dots & \dots \end{vmatrix}. \tag{8}
$$

We can then evaluate the transfer of any initial mixed state $\rho_a = \sum_{\vec{p},\vec{q}} a_{\vec{p}\vec{q}} |\vec{p}\rangle\langle\vec{q}|$ to another mixed state ρ_b by calculating the relevant correlation between the evolved state and the final desired state,

$$
M_{ab}(t) = \sum_{\vec{r},\vec{s},\vec{p},\vec{q}} b_{\vec{r}\vec{s}} a_{\vec{p}\vec{q}} A_{\vec{p}\vec{r}}(t) A^*_{\vec{q}\vec{s}}(t). \tag{9}
$$

It is important to stress that the above expressions allow us to calculate the evolution of an *arbitrary* mixed state for *any* choice of couplings in the *XX* Hamiltonian of Eq. (1), as we only used the property that this Hamiltonian describes noninteracting fermions.[1] Thus, the higher excitations are seen to propagate simultaneously at the same group velocity. This result can be used to search for coupling distributions that give better state transfer properties than the equal-coupling case. In particular, because the transfer of the one-spin polarization state $\delta\rho_z^j$ is found to have the same expression as the spin-excitation state transfer, we can use known results for the latter to find optimal coupling distributions.

C. Perfect state transfer for engineered Hamiltonians

Although spin excitations propagate through the chain for any *XX* Hamiltonian, as seen in the homogeneous case this does not always allow for perfect state transfer because of wave-packet dispersion [25,26]. Good transport properties have been found for a class of Hamiltonians that have been suitably engineered, either by modifying the coupling strengths among the spins or by introducing an additional spatially varying magnetic field [6,27]. In particular, the Hamiltonian

$$
\mathcal{H}^o_{XX} = \sum_{j=1}^{n-1} 2d\sqrt{\frac{j(n-j)}{n^2}} (\sigma_+^j \sigma_-^{j+1} + \sigma_-^j \sigma_+^{j+1}) \tag{10}
$$

allows for optimal transport of the excitation from the first to the last spin in the chain. Not only does this choice of couplings allow for perfect transport [6,28,29], but it does so in the shortest time [30,31]. Notice that in Eq. (10) we expressed the couplings in terms of the maximum coupling constant d, since typically this will be constrained in experimental implementations, as opposed to the more common choice in the literature, whereby $d_j = \frac{d'}{2}\sqrt{j(n-j)}$, with $d' = 4d/n$.

---

[1]For some states having a simple form in fermionic operators, it might instead be advantageous to calculate the transport correlation functions directly [7,80].

The optimal coupling Hamiltonian $\mathcal{H}^o_{XX}$ can be diagonalized by the following fermion operators [32,33]:

$$
a^o_k = \sum_j \alpha_j(k) c_j,
$$

$$
\alpha_j(k) = 2^{\frac{n+1}{2}-j} \sqrt{\frac{k}{j}\binom{n}{k}\bigg/\binom{n}{j}} J_{n-j}^{(j-k,j+k-n-1)}, \tag{11}
$$

where $J_n^{(a,b)}$ is the Jacobi polynomial evaluated at 0. The eigenvalues read $\omega_k^o = \frac{2d}{n}[2k - (n+1)]$. The transfer amplitude $A_{jl}^{o,XX}(t)$ between spin j and spin l then becomes $A_{jl}^{o,XX}(t) = \sum_k \alpha_j(k)\alpha_l(k)e^{-i\omega_k^o t}$, which yields the transfer function $P_{jl}^{o,XX}(t) = |A_{jl}^{o,XX}(t)|^2$. Using these results, we can calculate the transfer probability from spin 1 to spin n of the one-spin excitation in a pure-state chain,

$$
P_{1n}^{o,XX} = [\sin(\tau)]^{2(n-1)}, \quad \tau = \frac{4dt}{n}. \tag{12}
$$

The same expression also describes the transport of the spin-polarization ($\delta\rho_z^j$) in a mixed-state chain. Notice that at a time $t^\star = \frac{\pi}{2}\frac{n}{4d}$, perfect transfer is achieved. This optimal time reflects the maximum speed of the transport, which is given by the group velocity, $v_g = 4d\frac{2}{\pi}$, of the spin wave traveling through the chain [25,26].

Perfect state transfer is achieved not only for the choice of couplings in Eq. (10) but, more generally, for a class of *XX* Hamiltonians that supports either a linear or a quadratic spectrum [34–37]. It was observed that these Hamiltonians allow for perfect mirror inversion of an arbitrary (pure) input state. A different approach to perfect pure-state transfer, with a generic Hamiltonian spectrum, is to confine the dynamics of the system to an effective two-qubit subspace [38–40] (which by construction is always mirror-symmetric) or to restrict the evolution between two or three quasiresonant eigenvectors [15,41,42]. The confinement is obtained by weakening the couplings of the first and last qubit in the chain. This approach has been shown to achieve perfect transfer with the Hamiltonian in Eq. (1), even for mixed-state chains [15] and in the presence of disorder in the couplings [15,38], provided that $d_1, d_{n-1} \ll d_i$. The scheme could be applied as well to the Hamiltonian discussed in the next section [Eq. (13)]. For more general long-range Hamiltonians, such as the *XXZ* dipolar Hamiltonian considered in [38,39], the equivalence of the evolution between pure and mixed state is lost and it is thus not possible to directly apply this strategy.

D. Transport via double-quantum Hamiltonian

In the previous sections we showed that the transport features of *XX* Hamiltonians relied on the mapping to free fermions and the conservation of spin (or magnon) excitation number. It is therefore surprising to find other classes of Hamiltonians that show very similar transport properties, even if they do not conserve the number of single-spin
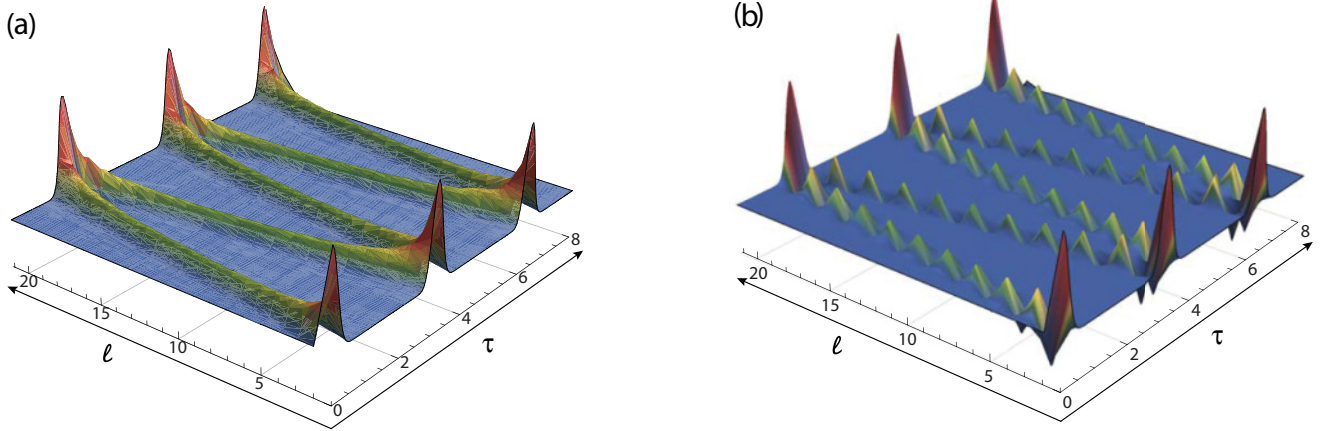
FIG. 1. (Color online) (a) Transport of polarization under the *XX* Hamiltonian with optimal couplings [Eq. (10)]. Shown is the intensity of the polarization at each spin site $C_{1,\ell}^{o,XX}(t) = P_{1,\ell}^{o,XX}(t)$ as a function of normalized time $\tau = 4dt/n$ for a propagation starting from spin 1. The chain length $n = 21$ spins. (b) Transport of polarization under the double-quantum Hamiltonian $C_{1,\ell}^{o,\mathsf{DQ}}(t)$ [Eq. (14)], with the same parameters as in (a).

excitations. Consider the so-called double-quantum (DQ) Hamiltonian,

$$\mathcal{H}_{\mathsf{DQ}} = \sum_j \frac{d_j}{2} \left(\sigma_x^j \sigma_x^{j+1} - \sigma_y^j \sigma_y^{j+1} \right)$$

$$= \sum_j d_j \left(\sigma_+^j \sigma_+^{j+1} + \sigma_-^j \sigma_-^{j+1} \right). \tag{13}$$

As this Hamiltonian does not conserve the spin excitation number, $[\mathcal{H}_{\mathsf{DQ}}, Z] \neq 0$, we would not expect it to support the transport of single-spin excitations. However, as observed in [7,43], the DQ Hamiltonian is related to the *XX* Hamiltonian by a simple similarity transformation, $U_{\mathsf{DQ}}^{XX} = \prod_j \sigma_x^{2j+1}$. Therefore, the DQ Hamiltonian commutes with the operator $\tilde{Z} = \sum_j (-1)^{j+1} \sigma_z^j$ and can be block-diagonalized following the subspace structure defined by the (degenerate) eigenvalues of $\tilde{Z}$.[2] The DQ Hamiltonian allows for the mirror inversion of states contained in each of the subspaces defined by the eigenvalues of $\tilde{Z}$ (the equivalent of single-spin excitation and higher excitation manifolds for Z). For pure states, these states do not have a simple interpretation as local spin excitation states, and the DQ Hamiltonian is thus of limited practical usefulness for state transfer. Interestingly, however, the situation is more favorable for the transport of spin polarization in mixed-state chains. Indeed, states such as $\delta\rho_z^j$ are invariant, up to a sign change, under the similarity transformation U_{DQ}^{XX}. Thus we can recover the results obtained for the polarization transport under the *XX* Hamiltonian for any coupling distribution:

$$C_{jl}^{\mathsf{DQ}}(t) = (-1)^{j-l} |A_{jl}^{XX}(t)|^2. \tag{14}$$

In Fig. 1 we illustrate the transport of polarization from spin $j = 1$ as a function of the spin number ℓ and time. Comparing Fig. 1(a) with Fig. 1(b), which show the transport under the

optimal coupling *XX* and DQ Hamiltonian, respectively, we see enhanced modulations due to the positive-negative alternation of the transport on the even-odd spin sites. Despite this feature, perfect transport is possible even with the DQ Hamiltonian, which unlike the *XX* Hamiltonian, can be easily obtained from the natural dipolar Hamiltonian with only collective control [44,45].

III. PROTOCOL FOR MIXED-STATE QUANTUM-INFORMATION TRANSPORT

In the previous section we showed that mixed-state chains have transport properties similar to pure-state chains, as in both cases transport relies on the characteristics of the Hamiltonian (e.g., conservation of excitation number, mirror symmetry,...). However, while a pure eigenstate of the Z operator is transported using a mixed-state chain, coherences are not. This means that it is possible to transfer a bit of *classical* information by encoding it in the $|0\rangle$ and $|1\rangle$ states of the first spin in the chain, and that the same result can be obtained by encoding the information in the *sign* of the polarization using the states $\delta\rho_\pm = \pm\sigma_z^1$. This encoding is not enough, however, to transfer quantum information: this would require the additional transfer of information about the phase coherence of a state, for example, by transporting a state $\delta\rho_\pm = \pm\sigma_x^1$. The problem is that evolution of this state creates a highly correlated state, as σ_x^1 evolves to $\prod_{i=1}^{n-1} \sigma_z^i \sigma_\alpha$, where $\alpha = x(y)$ for n odd (even). Although particle-conserving Hamiltonians (such as the ones considered) allow for state transfer in any excitation manifold (and mirror-symmetric Hamiltonians achieve perfect state transfer), a manifold-dependent phase is associated with the evolution [46–49], and thus only states residing entirely in one of these manifolds can be transferred.

Information can be extracted from the resulting highly correlated state only with a measurement [13], at the cost of destroying the initial state and of introducing classical communication and conditional operations. Alternatively, a simple two-qubit encoding allows for the transport of a bit of quantum information [14]. For evolution under the *XX* Hamiltonian,

---

[2]Different non-spin-excitation conserving Hamiltonians have been proposed in [8,9,13], taking advantage of other conserved quantities.
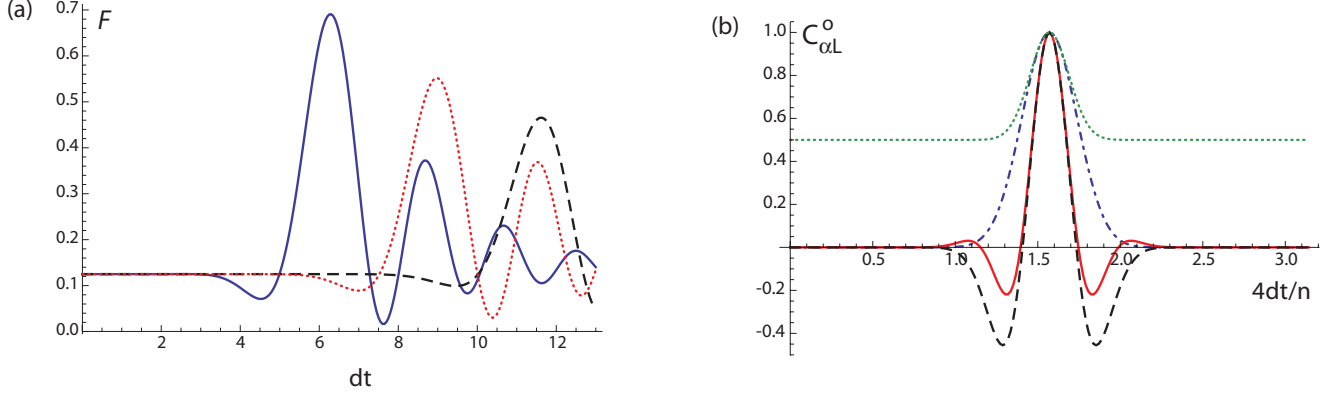
FIG. 2. (Color online) Transport of the four logical states as a function of time (normalized by the coupling strength). (a) Entanglement fidelity, $F = \frac{1}{4}\sum_\alpha C_{\alpha L}^h$, for the transport under the homogeneous *XX* Hamiltonian, for chains of $n = 10$ (blue, solid line), 15 (red, dotted line), and 20 (black, dashed line) spins. (b) Transport of the four logical basis states under the engineered optimal-coupling *XX* Hamiltonian in a 20-spin chain. σ_{xL}: Blue, dash-dotted line. σ_{yL}: Black, dashed line. σ_{zL}: Red, solid line. $\mathbb{1}_L$: Green, dotted line.

such encoding corresponds to the zero-eigenvalue subspace of the operator $\sigma_z^1 + \sigma_z^2$. A possible choice of logical qubit observables is given by

$$\sigma_{xL}^{XX} = \frac{\sigma_x^1\sigma_x^2 + \sigma_y^1\sigma_y^2}{2} \qquad \sigma_{yL}^{XX} = \frac{\sigma_y^1\sigma_x^2 - \sigma_x^1\sigma_y^2}{2}$$
$$\sigma_{zL}^{XX} = \frac{\sigma_z^1 - \sigma_z^2}{2} \qquad \mathbb{1}_L^{XX} = \frac{\mathbb{1} - \sigma_z^1\sigma_z^2}{2}, \qquad (15)$$

which corresponds to an encoded pure-state basis $|0\rangle_L^{XX} = |01\rangle$ and $|1\rangle_L^{XX} = |10\rangle$. If we perform the transport via the DQ Hamiltonian, the required encoding is instead given by the basis $|0\rangle_L^{DQ} = |00\rangle$ and $|1\rangle_L^{DQ} = |11\rangle$, as follows from the similarity transformation between *XX* and DQ Hamiltonians. Accordingly, the operator basis for the transport via mixed states under the DQ Hamiltonian is

$$\sigma_L^{DQ} = \frac{\sigma_x^1\sigma_x^2 - \sigma_y^1\sigma_y^2}{2} \qquad \sigma_{yL}^{DQ} = \frac{\sigma_y^1\sigma_x^2 + \sigma_x^1\sigma_y^2}{2}$$
$$\sigma_{zL}^{DQ} = \frac{\sigma_z^1 + \sigma_z^2}{2} \qquad \mathbb{1}_L^{DQ} = \frac{\mathbb{1} + \sigma_z^1\sigma_z^2}{2}. \qquad (16)$$

We can calculate the transport functions $C_{\alpha L}(t)$, $\alpha = \{x, y, z, \mathbb{1}\}$, from the overlap of the evolved state with the desired final state. For example, for *XX* transport this yields expressions of the form

$$C_{yL}(t) = \frac{1}{2}\text{Tr}\{U_{XX}(t)\sigma_{yL}^{XX}U_{XX}^\dagger(t)(\sigma_y^n\sigma_x^{n-1} - \sigma_x^n\sigma_y^{n-1})\}.$$

For the homogenous *XX* Hamiltonian we find

$$C_{1L}^h(t) = \frac{1}{2}\{1 + [A_{1,n-1}^h(t)A_{2,n-1}^h(t) - A_{1,n}^h(t)A_{2,n}^h(t)]^2\},$$
$$C_{(x,y)L}^h(t) = \frac{2(\pm 1)^{n+1}}{(n+1)^2}\sum_{k,h}(-1)^{h+k}e^{it(\omega_h \mp \omega_k)}$$
$$\times [\sin(2\eta)\sin(\kappa) + \sin(\eta)\sin(2\kappa)]^2,$$
$$C_{zL}^h(t) = \frac{1}{2}[P_{1,n}^{h,XX}(t) - 2P_{1,n-1}^{h,XX}(t) + P_{2,n-1}^{h,XX}(t)], \quad (17)$$

where we have defined $\eta = \pi h/(n+1)$. Note that the same expressions hold for the evolution of the states in Eq. (16) under the DQ Hamiltonian.

The transport under the homogenous Hamiltonians is, however, imperfect, not only because the transfer fidelity of each basis state is less than 1, but also because the maximum values occur at slightly different times. In Fig. 2 we plot the reduced entanglement fidelity [50,51] of such a transport process, computed as $F(t) = \frac{1}{4}\sum_\alpha C_{\alpha L}^h(t)$, for chains of different lengths.

The transport of the logical states under the engineered Hamiltonian $\mathcal{H}_{XX}^o$ with optimal couplings is given by

$$C_{1L}^o(t) = \frac{1}{2}[1 + \sin(\tau)^{4(n-2)}],$$
$$C_{xL}^o(t) = \sin(\tau)^{2(n-2)},$$
$$C_{yL}^o(t) = \sin(\tau)^{2(n-2)}[1 - 2(n-1)\cos^2(\tau)], \qquad (18)$$
$$C_z^o = \frac{1}{2}\{\sin(\tau)^{2(n-3)}[(n-1)\cos^2(\tau) - 1]^2$$
$$+ \sin(\tau)^{2(n-1)} - 2(n-1)\cos^2(\tau)\sin(\tau)^{2(n-2)}\}.$$

At the time $t^\star$ defined in Sec. II C the basis states are transported with fidelity 1. It is then possible to transfer an arbitrary state with unit fidelity (Fig. 2). Note that because of the interplay of the mirror inversion operated by the Hamiltonian and the similarity transformation between the *XX*- and DQ-Hamiltonians, an additional operation is needed to obtain perfect transport with the latter Hamiltonian. Specifically, for chains with an even number of spins, a π rotation around the x axis is required, which can be implemented on the whole chain or on the last two spins encoding the information. As this is a collective rotation, independent of the state transported, arbitrary state transfer is still possible.

The above encoding protocol can be extended to more than a single logical qubit, for example, by encoding an entangled state of two logical qubits into four spins [52,53], such as an encoded Bell state $|\psi\rangle = (|01\rangle_L + |10\rangle_L)/\sqrt{2}$. Provided that the extra encoding overhead can be accommodated, this will in principle allow perfect transport of entanglement through a completely mixed chain.

Altogether, these results point to a strategy for perfect transport in spin wires, without the need of initialization or control, but only exploiting control in a two-qubit (possibly four-qubit) register at each end of the wire. The simplicity

of such a protocol opens the possibility for experimental implementations, as we discuss next.

IV. EXPERIMENTAL PLATFORMS

While many theoretical advances have been made in the study of information transfer in spin chains, experimental implementations are still limited. Since departures from the idealized theoretical models (due, for instance, to long-range couplings, the presence of a bath or variations in the coupling strengths) make real systems much more complex to analyze analytically, experimental investigations able to study these issues are needed. Studying quantum-transport properties in highly mixed spin chains thus serves a dual purpose. First, the similarities of transport properties of pure and mixed states makes the latter a good test-bed for experiment. Second, protocols for perfect state transfer via mixed-state quantum wires allow us to relax some of the requirements for QIP architectures.

Mixed-state spin chains are encountered in a number of physical applications. Examples range from phosphorus defects in silicon nanowires [18] to quantum dots [16,28], from polymers such as polyacetylene [54] and other molecular semiconductors [55] to solid-state defects in diamond or silicon carbide [56,57]. In particular, the completely mixed-state chain studied here, corresponding to the infinite temperature limit, may often be a better approximation to the thermal states of these systems than low-temperature thermal states that may be viewed as perturbations to the ground state.[3]

In what follows, we describe two experimental platforms that best exemplify the advantages of transport via mixed-state chains.

A. Simulations in solid-state NMR systems

Recently, nuclear spin systems in apatite crystals have emerged as a test-bed to probe quasi-one-dimensional (1D) dynamics, including transport and decoherence [19,20,26,58,59]. Because the nuclear spins in apatites are found in a highly mixed state at room temperature, they are particularly well-suited to the protocol for quantum-information transport outlined in the previous section. NMR techniques enable this exploration even in the absence of single-spin addressing and readout.

The crystal structure of fluorapatite [$Ca_5(PO_4)_3F$] and hydroxyapatite [$Ca_5(PO_4)_3(OH)$] presents a favorable geometry where ^{19}F or ^1H nuclear spins are aligned in linear chains along the crystal c axis with interspin spacings much shorter than the distance to other parallel chains. In a sufficiently strong magnetic field, the nuclear spins interact via the *secular dipolar Hamiltonian* [44],

$$\mathcal{H}_{\text{DIP}} = \sum_{j<l}^{n} d_{jl} \left[\sigma_z^j \sigma_z^l - \frac{1}{2} \left(\sigma_x^j \sigma_x^l + \sigma_y^j \sigma_y^l \right) \right], \quad (19)$$

where the couplings depend on the relative positions as $d_{jl} = (\mu_0/16\pi)(\gamma^2\hbar/r_{jl}^3)(1 - 3\cos^2\theta_{jl})$, with μ_0 being the standard magnetic constant, γ the gyromagnetic ratio, r_{jl} the distance between nucleus j and l, and θ_{jl} the angle between $\vec{r}_{jl}$ and the z axis, respectively. The apatite geometry gives a ratio of intrachain to interchain couplings of about 40, allowing the evolution to approximate well the expected 1D dynamics over sufficiently short time scales [20].

Known pulse sequences [45,60,61] are able to synthesize the DQ Hamiltonian from the secular dipolar Hamiltonian. Furthermore, by relying on the symmetry breaking due to defects and on incoherent control, we showed in Ref. [19,20] how to prepare the initial state of relevance for polarization transport, $\delta\rho_z^{1,n} \propto \sigma_z^1 + \sigma_z^n$. (Notice that because of the symmetries in the chain and control Hamiltonians, it is not possible to prepare the state $\delta\rho_z^1 \propto \sigma_z^1$.)

Similar control protocols can be used to prepare other states for the transport of quantum information. Specifically, we want to prepare states such as σ_{xL}^{DQ} and σ_{yL}^{DQ}. To do so, one can first prepare the state $\delta\rho_z^{1,n}$ and then let the system evolve under the DQ Hamiltonian for a short time.[4] A so-called double-quantum filter then selects the desired state, $\delta\rho_y^L \propto \sigma_{yL}^{\text{DQ}}|_{1,2} + \sigma_{yL}^{\text{DQ}}|_{n-1,n}$, that is,

$$\delta\rho_y^L \propto \left(\sigma_y^1\sigma_x^2 + \sigma_x^1\sigma_y^2 \right)/2 + \left(\sigma_y^{n-1}\sigma_x^n - \sigma_x^{n-1}\sigma_y^n \right)/2. \quad (20)$$

Similarly, a $\pi/4$ collective rotation around z, prior to the double-quantum filter, is needed to select the $\delta\rho_x^L$ operator. The double-quantum filter is a form of temporal averaging [62], consisting of phase shifts of the pulse sequences in successive experiments. When averaging the experimental results, such phase shifts cancel out contributions to the signal arising from states outside the double-quantum coherence manifold. Similar techniques are well established in NMR [63] and have been used to study transport in fluorapatite [19].

A suitable metric of transport would then be given by the correlation of the evolved state with the initial state, $\mathcal{C}(t) = \text{Tr}\{\delta\rho(t)\delta\rho(0)\}$, since this contains the usual transfer terms (correlation of the evolved state with the desired final state at the chain end, $\text{Tr}\{\sigma_{yL}^{\text{DQ}}(t)|_{1,2}\, \sigma_{yL}^{\text{DQ}}|_{n-1,n}\}$). Even if the techniques just outlined are able to prepare the desired initial state, single-spin detection is not possible in conventional NMR, preventing quantum-information transport to be directly measurable. Still, there exist other signatures that reliably indicate when the transport from one end of the chain to the other has occurred. These signatures can be extracted experimentally from the measurement of collective magnetization, via so-called multiple-quantum NMR techniques [44,61]. These techniques are extremely useful to probe multispin processes and gain insight into many-body spin dynamics [45,58,61,64], as they reveal the multiple-quantum coherence (MQC) intensities of a spin state, thus effectively allowing a partial state tomography.

---

[3]As seen from studies of coherence time with polarization [81,82], many properties do not depend linearly on the deviation from the pure state.

[4]A time $t \approx 1.5/d$ is found to maximize the fidelity of the prepared state.

The nth-order MQC signal (when the observable is the total magnetization Z) is given by

$$\mathcal{J}_\rho^n(t) = \mathcal{F}_\varphi\{\text{Tr}[e^{-i\varphi_n Z}U(t)\rho(0)U(t)^\dagger e^{i\varphi_n Z}$$
$$\times U(t)ZU(t)^\dagger]\}, \qquad (21)$$

where $\mathcal{F}_\varphi\{\cdot\}$ is the Fourier transform with respect to the phase φ, and $U(t)$ is evolution under the DQ Hamiltonian [45]. For an arbitrary initial state $\rho(0)$, this corresponds to

$$\mathcal{J}_\rho^n(t) = \text{Tr}\{\mathcal{P}_n[\rho_j(t)]\mathcal{P}_{-n}[U(t)ZU(t)^\dagger]\}, \qquad (22)$$

where $\mathcal{P}_n[\cdot]$ denotes the projector onto the $+n$ coherence manifold.

Although in three-dimensional (3D) systems high coherence orders can be created, the 1D, nearest-neighbor DQ Hamiltonian creates only two-spin excited states (zero- and double-quantum coherences), and thus it does not populate higher coherence order manifolds [65]. Furthermore, it was observed in Ref. [7] that upon preparation of the state relevant for transport, $\delta\rho_z^{1,n}$, the zero- and double-quantum intensities $\mathcal{J}_z^{0,2}(t)$ produced a clear signature of the transport.

In the nearest-neighbor approximation, with $d = -\mu_0\gamma^2\hbar/(8\pi r_{nn}^3)$ and r_{nn} being the nearest-neighbor distance, the MQC intensities can be calculated analytically, in the form

$$\mathcal{J}_z^{0,2}(t) = \frac{\alpha_{0,2}}{n+1}\sum_{k=1}^n \sin^2(\kappa)\cos^2(2\omega_k t + \phi_{0,2}), \qquad (23)$$

where $(\phi_0 = 0, \alpha_0 = 2)$ for the zero-quantum and $(\phi_2 = \frac{\pi}{2}, \alpha_2 = 1)$ for the double-quantum intensities, respectively. Similarly, we can calculate the MQC intensities for the initial states corresponding to $\delta\rho_{x,y}^L$ and evolving under the DQ Hamiltonian. Using the transformation to Bogoliubov operators [19], we obtain

$$\mathcal{J}_{yL}^{0,2}(t) = \frac{\alpha_{0,2}}{n+1}\sum_{k=1}^n \sin(\kappa)\sin(2\kappa)\sin(4\omega_k t + 2\phi_{0,2}), \qquad (24)$$

whereas the state $\delta\rho_x^L$ gives a zero signal.

In Fig. 3 we compare the transport metric $\mathcal{C}(t)$ with the MQC intensities $\mathcal{J}^0(t)$. A signature of transport from one end of the chain to the other is apparent in the coherence intensities. The observed local maxima in the MQC intensities

at the *mirror time* $t^* \sim n/(2d)$ [20] is due to constructive interferences when the propagation has traveled the length of the chain and is reflected back [26]. The MQC signature would be amenable to experimental tests in solid-state NMR systems by following the distinctive features of the MQC evolution. Other, more comprehensive forms of state tomography [66] inspired by MQC techniques could eventually be used to gather more information about the evolved state.

B. A quantum-computing architecture in diamond

We now turn to a promising implementation [15,23] of the protocol for perfect quantum-information transfer described in Sec. III. Distributed quantum-computing schemes [1–3] could play an important role in recently proposed solid-state quantum-computing architectures based on defects in diamond. The nitrogen-vacancy (N-V) center in diamond has emerged as an ideal qubit candidate [22,67,68], thanks to its long coherence times and the possibility of optical initialization and readout even at room temperature. This defect can be created by implanting nitrogen defects in diamond and allowing vacancies to recombine with them at high temperature. While nitrogen implantation can be done with high precision [69–72], the nitrogen to N-V conversion is limited. The remaining nitrogen defects ($P1$ centers [73]) are electronic spin 1/2 that can be used as quantum wires to connect the N-V–center qubits, as suggested in Refs. [15,23,74]. While N-V centers can be initialized to their ground state and controlled individually by a combination of microwave and optical control [75], the $P1$ centers will be found in a highly mixed state and will only be able to be controlled collectively.

The ideas developed in the previous sections find an ideal implementation in this engineered QIP system at room temperature. Control of the N-V centers at each end of the chain allows creation of the logical states [Eq. (16)] comprising the first neighboring $P1$ center. (Notice that control on just the end-chain spin could allow full controllability of the chain [11,12], although this might be inefficient [10,76].)

The nitrogens could be implanted at separations $r_{i,i+1} = r_{\min}\frac{(n/2)^{1/3}}{[j(n-j)]^{1/6}}$, with $r_{\min}$ being the minimum separation, in such a way that the couplings follow the ideal distribution that yields optimal transport. Although the implantation precision is low at present, technological
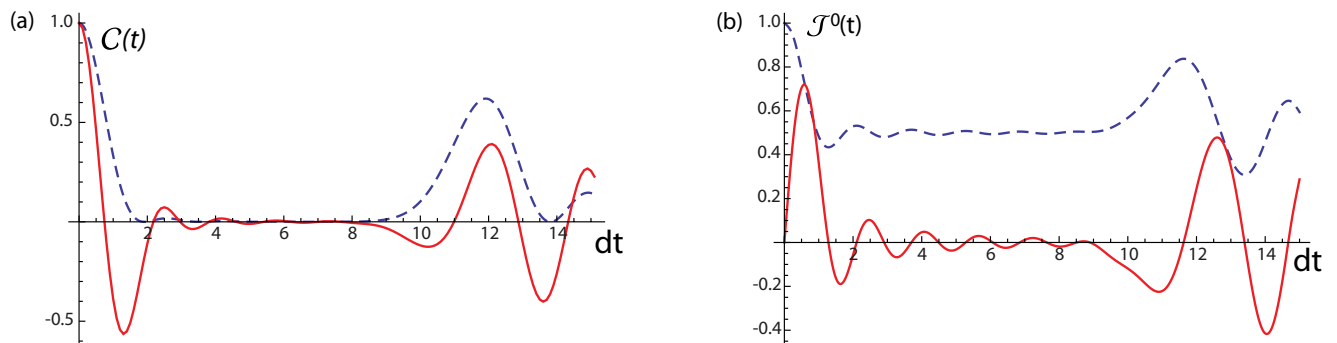

FIG. 3. (Color online) Transport of single-spin polarization $\delta\rho_z^{1,n}$ (blue, dashed) and logical-y state $\delta\rho_y^L$ (red), Eq. (20), in a $n = 21$-spin chain. (a) Correlation of the evolved state with the initial state, $\mathcal{C}(t) = \text{Tr}\{\rho(t)\rho(0)\}$, which also indicates transport from one end of the chain to the other. (b) Zero quantum coherence intensities for the two initial states.

advances should be able to reach the regime where the transfer protocol becomes robust against errors in the coupling strength [77]. The $P1$ centers will then interact via the dipolar interaction, which can be truncated to its secular part [Eq. (19)] at high enough magnetic fields (in practice less than ≈ 100 Gauss, for a minimum distance between nitrogens $r_{\min} \sim 15$ nm, corresponding to a coupling strength of ≈ 15 kHz).

Using multiple pulse sequences [45], the dipolar Hamiltonian is modulated into the DQ Hamiltonian that we have shown allows for perfect state transfer. At the same time, the pulse sequence refocuses the hyperfine interaction with the nitrogen nuclear spin,[5] as well as the coupling to the quasistatic ^{13}C nuclear spin-bath. Assuming a 5% error in the nitrogen positioning, chains of $n \sim 15$ spins with minimum separation of 15 nm would allow for information transport in about $t^{\star} = 200$ μs with high fidelity [30,77]. Local operations at the N-V center, enhanced by a register of nuclear spins [22], would allow for quantum error correction, while the separation between N-V centers achieved thanks to the $P1$ wires would enable individual addressing of the N-V qubits by subdiffraction-limit optical techniques [75,78]. Ultimately, this scheme could then serve as the basis for a scalable, room-temperature quantum computer [15,23].

V. CONCLUSIONS

We have investigated the properties of quantum-information transport in mixed-state spin chains. Focusing, in particular, on the infinite temperature limit, we have identified strong similarities between pure- and mixed-state transport. These similarities enable the simulation of pure-state transport properties using more readily accessible high-temperature mixed states. Specifically, we could apply results derived for pure-state transport to achieve perfect state transfer with an engineered XX Hamiltonian. Other recently proposed schemes, involving, for instance, weaker couplings of the chain ends [39,40] or modulation of an external bias magnetic field [79], should be further explored to determine under which conditions they could be extended to mixed-state chains with different coupling topologies. More generally, it would be interesting to investigate the wave-dispersion properties [25] of mixed-state chains versus pure-state chains, as mixed-state systems are ubiquitous in experimental implementations.

In this paper we have discussed in particular a potential experimental platform provided by apatite crystals controlled by NMR techniques. Experimental simulations of pure-state transport would allow exploring the effects of disordered and long-range couplings, interaction with an environment, and other nonidealities that are bound to appear in practical implementations and that are not amenable to direct analytical and/or numerical studies.

Furthermore, it becomes possible to use known results of pure-state transport to devise protocols for perfect spin transfer, even using highly mixed states. Specifically, we have shown that combining a simple encoding of the transmitted state into one or more spin pairs with engineered couplings in the chain allows for the perfect transfer of quantum information and potentially of entanglement. An additional advantage of mixed-state chains is that they enable transport of relevant states via a non-spin-excitation conserving Hamiltonian, the DQ Hamiltonian, which can be obtained by coherent averaging from the naturally occurring magnetic dipolar interaction. These results have been combined to obtain a proposal for scalable quantum-computation architecture using electronic spin defects in diamond [15,21,23], which may be experimentally viable with existing or near-term capabilities.

---

[5]The refocusing is effective only in the presence of a large enough external magnetic field, when the hyperfine interaction reduces to its secular component. Otherwise, other decoupling techniques should be used.

---

[1] D. Burgarth, V. Giovannetti, and S. Bose, Phys. Rev. A **75**, 062327 (2007).

[2] L. Jiang, J. M. Taylor, A. S. Sørensen, and M. D. Lukin, Phys. Rev. A **76**, 062323 (2007).

[3] E. T. Campbell, Phys. Rev. A **76**, 040302(R) (2007).

[4] S. Bose, Phys. Rev. Lett. **91**, 207901 (2003).

[5] M. Christandl, N. Datta, A. Ekert, and A. J. Landahl, Phys. Rev. Lett. **92**, 187902 (2004).

[6] M. Christandl, N. Datta, T. C. Dorlas, A. Ekert, A. Kay, and A. J. Landahl, Phys. Rev. A **71**, 032312 (2005).

[7] P. Cappellaro, C. Ramanathan, and D. G. Cory, Phys. Rev. Lett. **99**, 250506 (2007).

[8] A. Kay, Phys. Rev. Lett. **98**, 010501 (2007).

[9] A. Kay, Int. J. Quantum. Inform. **8**, 641 (2010).

[10] D. Burgarth, K. Maruyama, M. Murphy, S. Montangero, T. Calarco, F. Nori, and M. B. Plenio, Phys. Rev. A **81**, 040303 (2010).

[11] J. Fitzsimons, L. Xiao, S. C. Benjamin, and J. A. Jones, Phys. Rev. Lett. **99**, 030501 (2007).

[12] J. Fitzsimons and J. Twamley, Phys. Rev. Lett. **97**, 090502 (2006).

[13] C. DiFranco, M. Paternostro, and M. S. Kim, Phys. Rev. Lett. **101**, 230502 (2008).

[14] M. Markiewicz and M. Wiesniak, Phys. Rev. A **79**, 054304 (2009).

[15] N. Y. Yao, L. Jiang, A. V. Gorshkov, Z.-X. Gong, A. Zhai, L.-M. Duan, and M. D. Lukin, Phys. Rev. Lett. **106**, 040505 (2011).

[16] Z. M. Wang, K. Holmes, Y. I. Mazur, and G. J. Salamo, Appl. Phys. Lett. **84**, 1931 (2004).

[17] J. Lao, J. Huang, D. Wang, and Z. Ren, Adv. Mater. **16**, 65 (2004).

[18] F. J. Ruess, W. Pok, T. C. Reusch, M. Butcher, K. E. Goh, L. Oberbeck, G. Scappucci, A. Hamilton, and M. Simmons, Small **3**, 563 (2007).

[19] P. Cappellaro, C. Ramanathan, and D. G. Cory, Phys. Rev. A **76**, 032317 (2007).

[20] W. Zhang, P. Cappellaro, N. Antler, B. Pepper, D. G. Cory, V. V. Dobrovitski, C. Ramanathan, and L. Viola, Phys. Rev. A **80**, 052323 (2009).

[21] P. Neumann *et al.*, Nat. Phys. **6**, 249 (2010).

[22] P. Cappellaro, L. Jiang, J. S. Hodges, and M. D. Lukin, Phys. Rev. Lett. **102**, 210502 (2009).

[23] N. Y. Yao, L. Jiang, A. V. Gorshkov, P. C. Maurer, G. Giedke, J. I. Cirac, and M. D. Lukin, e-print arXiv:1012.2864 [quant-ph].

[24] A. Bayat and S. Bose, Phys. Rev. A **81**, 012304 (2010).

[25] T. J. Osborne and N. Linden, Phys. Rev. A **69**, 052315 (2004).

[26] C. Ramanathan, P. Cappellaro, L. Viola, and D. G. Cory, eprint arXiv:1102.3400.

[27] C. DiFranco, M. Paternostro, D. I. Tsomokos, and S. F. Huelga, Phys. Rev. A **77**, 062337 (2008).

[28] G. M. Nikolopoulos, D. Petrosyan, and P. Lambropoulos, J. Phys. Condens. Matter **16**, 4991 (2004).

[29] G. M. Nikolopoulos, D. Petrosyan, and P. Lambropoulos, Europhys. Lett. **65**, 297 (2004).

[30] A. Kay, Phys. Rev. A **73**, 032306 (2006).

[31] M.-H. Yung, Phys. Rev. A **74**, 030303 (2006).

[32] B. Shore and J. Eberly, Opt. Comm. **24**, 83 (1978).

[33] R. J. Cook and B. W. Shore, Phys. Rev. A **20**, 539 (1979).

[34] C. Albanese, M. Christandl, N. Datta, and A. Ekert, Phys. Rev. Lett. **93**, 230502 (2004).

[35] T. Shi, Y. Li, Z. Song, and C.-P. Sun, Phys. Rev. A **71**, 032309 (2005).

[36] V. Kostak, G. M. Nikolopoulos, and I. Jex, Phys. Rev. A **75**, 042319 (2007).

[37] X. Q. Xi, J. B. Gong, T. Zhang, R. H. Yue, and W. M. Liu, Eur. Phys. J. D **50**, 193 (2008).

[38] G. Gualdi, V. Kostak, I. Marzoli, and P. Tombesi, Phys. Rev. A **78**, 022325 (2008).

[39] G. Gualdi, I. Marzoli, and P. Tombesi, New J. Phys. **11**, 063038 (2009).

[40] E. B. Fel'dman, E. I. Kuznetsova, and A. I. Zenchuk, Phys. Rev. A **82**, 022332 (2010).

[41] A. Wojcik, T. Luczak, P. Kurzynski, A. Grudka, T. Gdala, and M. Bednarska, Phys. Rev. A **72**, 034303 (2005).

[42] M. B. Plenio and F. L. Semiao, New J. Phys **7**, 73 (2005).

[43] S. Doronin, I. Maksimov, and E. Fel'dman, JETP **91**, 597 (2000).

[44] M. Munowitz and A. Pines, *Principles and Application of Multiple-Quantum NMR*, Adv. Chem. Phys. (Wiley, 1987), Vol. 66, pp. 1–152.

[45] C. Ramanathan, H. Cho, P. Cappellaro, G. S. Boutis, and D. G. Cory, Chem. Phys. Lett. **369**, 311 (2003).

[46] S. R. Clark, C. M. Alves, and D. Jaksch, New J. Phys. **7**, 124 (2005).

[47] S. R. Clark, A. Klein, M. Bruderer, and D. Jaksch, New J. Phys. **9**, 202 (2007).

[48] D. Burgarth, K. Maruyama, and F. Nori, Phys. Rev. A **79**, 020305(R) (2009).

[49] C. DiFranco, M. Paternostro, and M. S. Kim, Phys. Rev. Lett. **102**, 187203 (2009).

[50] E. M. Fortunato, L. Viola, J. Hodges, G. Teklemariam, and D. G. Cory, New J. Phys. **4**, 5 (2002).

[51] M. A. Nielsen, Phys. Lett. A **303**, 249 (2002).

[52] J. S. Hodges, P. Cappellaro, T. F. Havel, R. Martinez, and D. G. Cory, Phys. Rev. A **75**, 042320 (2007).

[53] M. K. Henry, C. Ramanathan, J. S. Hodges, C. A. Ryan, M. J. Ditty, R. Laflamme, and D. G. Cory, Phys. Rev. Lett. **99**, 220501 (2007).

[54] M. Nechtschein, F. Devreux, R. L. Greene, T. C. Clarke, and G. B. Street, Phys. Rev. Lett. **44**, 356 (1980).

[55] P. Petit and P. Spegt, J. Phys. (France) **51**, 1645 (1990).

[56] J. R. Weber, W. F. Koehl, J. B. Varley, A. Janotti, B. B. Buckley, C. G. Van de Walle, and D. D. Awschalom, Proc. Natl. Acad. Sci. USA **107**, 8513 (2010).

[57] J. Wrachtrup, Proc. Natl. Acad. Sci. USA **107**, 9479 (2010).

[58] H. J. Cho, P. Cappellaro, D. G. Cory, and C. Ramanathan, Phys. Rev. B **74**, 224434 (2006).

[59] E. Rufeil-Fiori, C. M. Sánchez, F. Y. Oliva, H. M. Pastawski, and P. R. Levstein, Phys. Rev. A **79**, 032324 (2009).

[60] M. Munowitz, A. Pines, and M. Mehring, J. Chem. Phys. **86**, 3172 (1987).

[61] J. Baum, M. Munowitz, A. N. Garroway, and A. Pines, J. Chem. Phys. **83**, 2015 (1985).

[62] E. Knill, I. Chuang, and R. Laflamme, Phys. Rev. A **57**, 3348 (1998).

[63] M. Rance, O. W. Sørensen, G. Bodenhausen, G. Wagner, R. R. Ernst, and K. Wthrich, Biochem. Biophys. Res. Commun. **117**, 479 (1983).

[64] H. J. Cho, T. D. Ladd, J. Baugh, D. G. Cory, and C. Ramanathan, Phys. Rev. B **72**, 054427 (2005).

[65] E. B. Fel'dman and S. Lacelle, J. Chem. Phys. **107**, 7067 (1997).

[66] J. D. van Beek, M. Carravetta, G. C. Antonioli, and M. H. Levitt, J. Chem. Phys. **122**, 244510 (2005).

[67] J. Wrachtrup and F. Jelezko, J. Phys. Condens. Matter **18**, S807 (2006).

[68] L. Childress, M. V. Gurudev Dutt, J. M. Taylor, A. S. Zibrov, F. Jelezko, J. Wrachtrup, P. R. Hemmer, and M. D. Lukin, Science **314**, 281 (2006).

[69] C. D. Weis *et al.*, J. Vac. Sci. Technol. B **26**, 2596 (2008).

[70] D. M. Toyli, C. D. Weis, G. D. Fuchs, T. Schenkel, and D. D. Awschalom, Nano Lett. **10**, 3168 (2010).

[71] B. Naydenov, V. Richter, J. Beck, M. Steiner, P. Neumann, G. Balasubramanian, J. Achard, F. Jelezko, J. Wrachtrup, and R. Kalish, Appl. Phys. Lett. **96**, 163108 (2010).

[72] P. Spinicelli *et al.*, e-print arXiv:1008.1483.

[73] R. Hanson, F. M. Mendoza, R. J. Epstein, and D. D. Awschalom, Phys. Rev. Lett. **97**, 087601 (2006).

[74] Bulletin of the American Physical Society, *41st Annual Meeting of the APS Division of Atomic, Molecular and Optical Physics*, Houston, Texas **55**, 5 (2010).

[75] P. C. Maurer *et al.*, Nat. Phys. **6**, 912 (2010).

[76] T. Caneva, M. Murphy, T. Calarco, R. Fazio, S. Montangero, V. Giovannetti, and G. E. Santoro, Phys. Rev. Lett. **103**, 240501 (2009).

[77] G. De Chiara, D. Rossini, S. Montangero, and R. Fazio, Phys. Rev. A **72**, 012323 (2005).

[78] E. Rittweger, D. Wildanger, and S. W. Hell, Europhys. Lett. **86**, 14001 (2009).

[79] G. A. Álvarez, M. Mishkovsky, E. P. Danieli, P. R. Levstein, H. M. Pastawski, and L. Frydman, Phys. Rev. A **81**, 060302 (2010).

[80] E. B. Fel'dman and S. Lacelle, Chem. Phys. Lett. **253**, 27 (1996).

[81] J. Fischer, M. Trif, W. Coish, and D. Loss, Solid State Commun. **149**, 1443 (2009).

[82] S. Takahashi, R. Hanson, J. van Tol, M. S. Sherwin, and D. D. Awschalom, Phys. Rev. Lett. **101**, 047601 (2008).